H1 alignment experience

C. Kleinwort[a]
for the H1 Collaboration

[a] Deutsches Elektronen-Synchrotron
D-22607 Hamburg, Germany

Abstract

This report describes the experience gained during alignment of the tracking system of the H1 detector. It concentrates on the alignment and calibration of the central trackers using the *Millepede* method for the reprocessing of the HERA I data in 2001/2002 and recent improvements for the HERA II data taking. The methods used by the other tracking detectors of H1 are mentioned only briefly.

5.1 H1 tracking system

The H1 detector [1] is a nearly hermetic multipurpose apparatus built to investigate high-energy electron–proton interactions at the HERA collider. The interaction point is surrounded by the forward, central, and backward tracking systems (see Fig. 5.1).

Fig. 5.1: Side view of the H1 tracking system

The tracking systems are placed in a liquid argon calorimeter, surrounded by a superconducting solenoid which provides a uniform magnetic field of 1.15 T parallel to the beam line and an instrumented iron return yoke acting as muon detector.

5.1.1 H1 central tracker

The main component of the central tracker (see Fig. 5.2) is the central jet chamber (CJC). This 220 cm long drift chamber consists of 56 layers of anode wires strung parallel to the beam axis in two separate rings covering radii from 20 to 85 cm. The inner ring (CJC1) is divided into 30 cells in the azimuthal direction, the outer ring (CJC2) into 60 cells. The cells are not pointing to the centre of the chamber but are rotated by about $30°$ to account for the Lorentz angle.
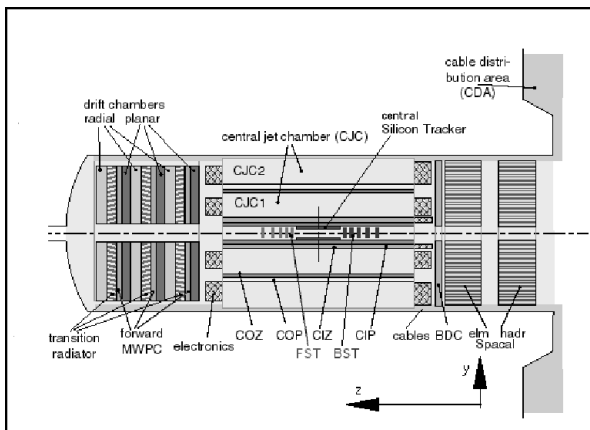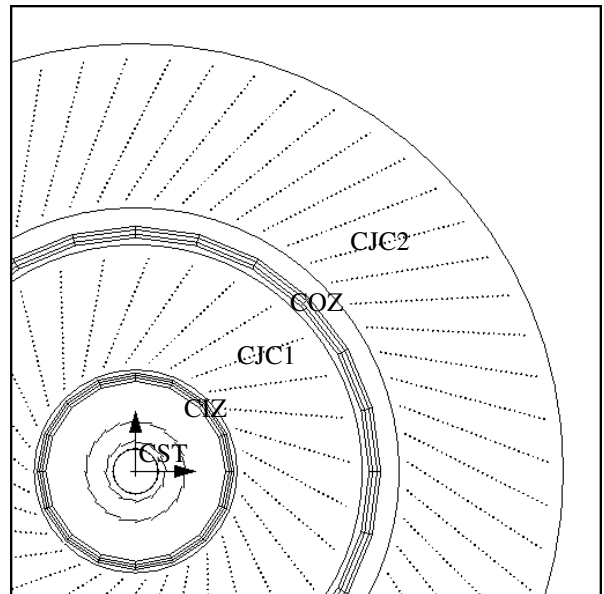

Fig. 5.2: Radial view of the H1 central tracker

The CJC allows a determination of the hit position in the $R\varphi$ plane perpendicular to the beam axis based on the measured drift time with a precision of

about $150\,\mu$m and a coarse determination of the Z position of the hit along the beam line using charge division with an accuracy of a few centimetres. It is supplemented by the central silicon tracker (CST) [2] to improve the track parameters at the vertex and additional drift chambers (CIZ, COZ) with the wires strung perpendicular to the beam axis on a 24-fold polygon for precise Z measurement. All chambers are operated at atmospheric pressure. For these detectors, tracking optimization means determination of the geometry ('*internal and external alignment*') and of the time-to-distance relation ('*calibration*').

The CST consists of 32 ladders of double-sided silicon strip detectors arranged in two concentric layers around the beam axis at radii of 6 and 10 cm. Each ladder is made of two half-ladders on which three sensors of 6 cm length are daisy chained and read out to one side. The strip pitch is 50 μm in $R\varphi$ and 88 μm in Z.

A track is described by a helix parameterized in $R\varphi$ by the curvature (κ), the distance of closest approach (to the origin) (d_{ca}) and the azimuth (φ_0) at the point of closest approach and in RZ by the z coordinate at the point of closest approach (Z_0) and the polar angle (θ) with respect to the proton direction.

5.2 Data sets and methods used

The large variety of track detectors requires various data sets and different alignment strategies for the determination of the optimal alignment and calibration constants.

5.2.1 Data sets

The ep collisions at HERA unfortunately do not provide clear calibration channels with simple topology which could be used for alignment. Instead a mixture of data sets has to be used which include

- Survey data from construction and installation of the tracking detectors.
- Tracks from ep interactions.
- Tracks from cosmic-ray muons ('*cosmics*'), which represent the dominant source for tracks with high momenta of several GeV with a trigger rate of 10–20 Hz in the central tracker. These events are typically taken in beam-off periods when it is easily possible to vary detector parameters like electrical or the magnetic field for systematic studies. Tracks from cosmic rays populate a different phase space than tracks from ep interactions (e.g., angular distributions, distance to interaction point and flight direction), which offers the opportunity for a number of systematic cross-checks.

5.2.2 Internal methods

Cosmic-ray muons taken with magnetic field switched off provide straight tracks which are used for the internal alignment of sub-detector modules of the forward tracker and the central and forward muon trackers.

5.2.3 External methods

In the event reconstruction the information of all tracking systems has to be combined. Therefore all precision detectors have to be aligned with respect to each other. The H1 convention uses the central tracker as frame of reference. For the alignment of various detectors relative to the central tracker the following methods are used:

- Central tracks for cosmics are extrapolated into the central muon tracker.
- For the measurement of the scattered electron in DIS events the backward silicon tracker uses the event vertex reconstructed from central tracks and central tracks which also pass through the BST. Cross-checks are done using kinematic constraints like comparing the momentum and the energy as measured in the backward calorimeter SpaCal (E/p).
- For tracks from ep interactions the track parameters measured by the forward drift chambers are compared to the central tracks.
- The forward and backward silicon trackers use a Kalman filter with the event vertex and central space points on tracks as input.

5.2.4 Combined methods

To reach optimal performance a large number of parameters are needed to describe all systematic effects occurring in the track detectors. Usually many of these parameters are strongly correlated. If not described properly most effects are absorbed in the track parameters, which leads to biased results. Therefore a combined procedure which allows simultaneous determination of alignment and calibration constants is used for the central trackers.

5.3 Millepede

For the alignment and calibration of the H1 central trackers the *Millepede* [3] method is used. It allows the determination of a large number of alignment and calibration parameters in a simultaneous linear least-squares fit of an arbitrary number of tracks accounting for the correlations between the global parameters to be measured and the local track parameters.

5.4 Reprocessing of HERA I data

At the end of the HERA I data-taking period (1992–2000) a coordinated alignment and calibration effort (1999–2001) was made in preparation for a major data reprocessing. Local corrections as well as the time stability in view of temperature and pressure variations were studied in detail.

5.4.1 Alignment and calibration in $R\varphi$

The purpose of the common alignment and calibration of central jet chambers and central silicon tracker was to determine local corrections to improve the measurement of transverse momentum p_t and distance of closest approach d_ca.

5.4.1.1 CJC $R\varphi$ measurement

From the measured drift time t, the time of the particle passage t_0, and the drift velocity v_d the drift distance d can be calculated. In most of the drift region the electric field configuration leads to isochrones, which in good approximation can be described by circles with constant radius R_iso. The drift distance d then in addition depends on the angle β between the normal to the drift and the flight direction of the particle:

$$d = (t - t_0)v_\mathrm{d} + R_\mathrm{iso}\left(\frac{1}{\cos\beta} - 1\right) . \quad (5.1)$$

Points in the $R\varphi$ plane (see Fig. 5.3) are determined from drift distance, drift direction according to the Lorentz angle α_lor, and the anode wire positions. Ambiguities are resolved by the pattern recognition.

$$(x, y) = (x_\mathrm{wire}, y_\mathrm{wire}) \pm d(\cos\alpha_\mathrm{lor}, \sin\alpha_\mathrm{lor}) . \quad (5.2)$$

5.4.1.2 Correlation between calibration and alignment constants

The importance of simultaneous determination of all parameters by correctly taking into account their correlations as done by *Millepede* is illustrated in the following example. Wire staggering and different gravitational sagging of anodes and cathodes lead to slightly different configurations of the electrical field and therefore different time-to-distance relations for the two drift sides of one anode. Neglecting these geometric effects in the calibration parameters would lead to different constants for drift time offsets for the two drift sides which have a similar effect to anode wire displacements in the drift direction.
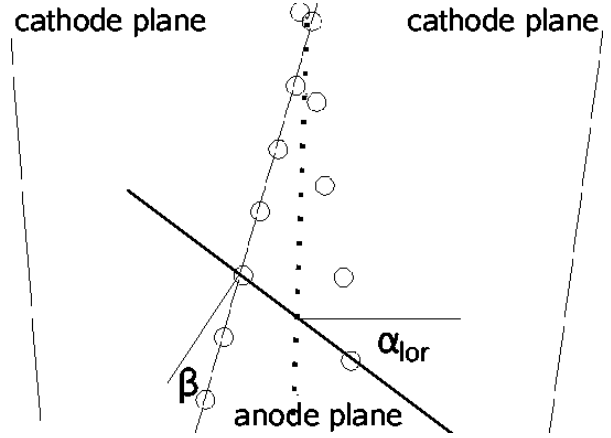

Fig. 5.3: CJC cell with track segment, drift direction and mirror hits

5.4.1.3 CST $R\varphi$ measurement

The local $R\varphi$ coordinates on a CST half-ladder are obtained from the centre of gravity of the cluster of the p-side strips hit and the position of the sensor on the half-ladder according to a microscope survey performed during assembly of the detector with an accuracy of a few microns. In the reconstruction the 3-fold Z ambiguity caused by the daisy chain readout can only be resolved by external information based on the extrapolation of CJC tracks.

5.4.1.4 Millepede set-up

5.4.1.4.1 Local track model

In the reconstruction a local track model is employed in which the hit residuals to an initial track fit are used as input. For cosmic events both track halves are fitted together after reversing the time-of-flight correction for the upper half. For data taken with magnetic field on, the track is parameterized as a parabola allowing for additional scattering angles due to the material between CST and CJC, which corresponds to approximately 1% of X_0. For cosmic tracks recorded without magnetic field a straight line is used as track model.

5.4.1.4.2 Global alignment parameter

The global alignment parameters, which completely define the positions of the 64 CST half-ladders ('*HL*') and the Z-dependent $R\varphi$-coordinates of the 2640 CJC anode wires, are listed in Table 5.1.

5.4.1.4.3 Global calibration parameter

The calibration accounts for the time variation of gas parameters, like pressure, temperature and composition as well as of space charge effects, spatial variations of the electrical field E, different cable length, and for

modifications in the readout electronics like exchange of FADC readout boards. A large number of calibration constants is required to parameterize such effects (see Table 5.2). An initial set of time-dependent calibration constants is already determined during the online calibration which is done on a processor farm as part of the online reconstruction. Azimuthal inhomogeneities are mainly caused by local chamber defects like broken wires, ageing, or defective high-voltage distribution. During HERA I running severe ageing problems [4] were observed in some regions of the CJC leading to operational problems and to strongly φ-dependent calibration constants.

Table 5.1: Meaning and quantity of global alignment parameters required to describe CJC and CST geometry

Detector part	Parameter set	#par.
CJC	Two rigid bodies (without ΔZ)	10
CJC	Torsion angle between end walls	2
CJC	Anode staggering	4
CJC	Anode electrostatic deflection	4
CJC	Anode gravitational sagging	4
CJC layer	Anode position correction	112
CST HL	64 rigid bodies (without ΔZ)	320

Table 5.2: Meaning and quantity of calibration parameters for CJC

Detector part	Parameter set	#par.
CJC	$v_{\mathrm{d}}, \alpha_{\mathrm{lor}}, t_0$ (gas)	6
CJC cell half	$v_{\mathrm{d}} (E(\varphi))$	180
CJC cell	$t_0 (E(\varphi))$	90
CJC layer half	$v_{\mathrm{d}} (E(R))$	112
CJC layer	$t_0 (E(R))$	56
CJC group	t_0 (readout)	330

Additional parameters are needed for special cases like dedicated systematic studies of isochrone radii, local defects, or inhomogeneities.

5.4.1.4.4 Constraints

For each set of local calibration parameters like $v_{\mathrm{d}}(\varphi)$ or $t_0(R)$, a constraint is defined which requires the weighted sum of the parameters to vanish. This reduces the correlation between the different parameter sets and allows one to easily remove a single parameter set for systematic studies without introducing large changes to the other parameters. The global calibration parameters containing the time dependence remain unchanged by construction of the constraints.

5.4.1.5 Millepede operation

5.4.1.5.1 Iterations

Non-linear effects require an iterative minimization procedure. In the first step internal *Millepede* iterations perform the outlier rejection and account for non-linear dependencies of measurements and parameters. In the second step *Millepede* is rerun using the results from the first iteration as starting values. Finally the track reconstruction is repeated with the updated correction parameters.

5.4.1.5.2 Data samples and their use

Typical data sets consisting of several 10^4 tracks are used for the calibration. Cosmic tracks which cover a large range of distances to the interaction point and have small curvature are used first. The results are cross-checked with tracks from ep collisions which populate a somewhat orthogonal phase space with full azimuthal coverage. Finally both sets are used simultaneously.

Straight tracks from cosmic data taken without magnetic field are well suited to check for effects producing curvature offsets such as a torsion angle between the CJC end walls.

5.4.1.6 Lessons learned

For a relatively complicated configuration of many track detectors with quite different systematics as in the case of H1, naturally a certain experience has to be gained before stable and reliable results can be obtained. Although the experience can certainly not be directly transferred to other detector systems it might still be useful to report a number of observations made in the case of H1.

5.4.1.6.1 Choice of reference system

Using the CST as absolute frame of reference resulted in large rotations of the CJC wire planes, which vanished by allowing for a global misalignment between the two detectors. On the other hand, when the CST was only used as relative reference, large torsion angles of the CJC end walls incompatible with the installation survey were obtained. At this point the frame of reference has been changed to CJC2 using the survey data of the precision bores in the end walls from the chamber construction in 1989. Aligning the CST with respect to this frame resulted in a radial 'shrinkage' of the CST by 40–60 μm. This effect could be explained by a systematic problem with the radial centre of gravity for the CST hits in the 300 μm thick silicon, but hasn't been fully resolved.

5.4.1.6.2 Influence of magnetic field inhomogeneities

For cosmic data taken without magnetic field, the end wall torsion angles are compatible with the installation survey and the wire positions with the survey of the precision bores in the end wall. In contrast, consistent results from data with magnetic field could only be obtained after the up-to 6% magnetic field inhomogeneities were taken into account in the track model.
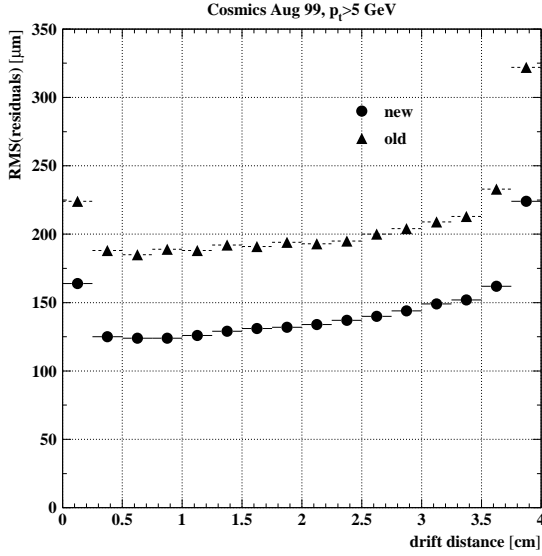

Fig. 5.4: CJC residuals in units of μm as a function of the drift distance (d). The anode is at $d = 0$ and the cathode in this case at $d = 4$ cm. The triangles are the values before and the circles after calibration and alignment with *Millepede*.

5.4.1.6.3 Cosmic versus ep tracks

It was observed that tracks from ep collisions with large curvature required t_0 corrections different from those obtained from cosmic tracks. This can be explained by the different distribution of the angle β between normal to drift direction and flight direction of these two event samples. For ep data the angle depends on the product of track curvature and (hit) radius while for cosmic tracks it rather is related to the distance to the interaction point divided by the (hit) radius. These differences have been resolved by additionally fitting the isochrone radius instead of using the trivial constant value of half the anode wire spacing times $\cos \alpha_{\mathrm{lor}}$.

5.4.1.7 Results

Applying all corrections described above the single hit resolution (see Fig. 5.4) and consequently the track parameter resolution for high momentum tracks have been improved by about a factor 1.5.

5.4.2 Alignment and calibration in ZS

To improve the measurement of the track parameters, Z-offset (Z_0) and polar angle (θ), a common alignment and calibration of CIZ, COZ and CST has been performed.

5.4.2.1 Millepede set-up

The use of *Millepede* for this application requires several adaptations.

5.4.2.1.1 Local track model

For the local track fit a straight line is used in the plane defined by Z and arc-length S. Only hits associated to tracks reconstructed in $R\varphi$ can be used because knowledge of the $R\varphi$ track parameters is needed to correct for the polygonal shape of CIZ and COZ and to obtain the relation between radius and arc-length.

5.4.2.1.2 Global alignment parameter

The global alignment parameters as listed in Table 5.3 completely define the positions of the CIZ and COZ anode wires. While in most of the phase space the COZ is used as frame of reference, the CST is used in the region where the detectors overlap. The Z alignment of the CST has been made internally before.

Table 5.3: Meaning and quantity of global alignment parameters used to describe wire positions of the central Z chambers

Detector part	Parameter set	#par.
CIZ	Rigid body (except $\Delta\varphi$)	5
COZ	Rigid body (except $\Delta\varphi$)	5
CIZ anodes	Offset in Z (16 rings with 4 wires)	64
COZ anodes	Offset in Z (24 rings with 4 wires)	96

5.4.2.1.3 Global calibration parameter

For each of the 160 anode wires v_{d} and t_0 corrections are determined.

5.4.2.2 Lessons learned

Again it might be useful to mention here specific observations made during ZS alignment and calibration.

5.4.2.2.1 Choice of reference system

While convergence has been reached whether CST or COZ were used as reference system, the results turned out to be inconsistent. With CST as reference the chambers had to be stretched by 0.5 ‰. Only after introducing the CST 'shrinkage' deduced from the $R\varphi$ alignment (see Section 5.4.1.6) did both choices of reference frame gave compatible values.

5.4.2.3 Results

Finally the single hit resolutions of the central Z chambers have been improved by about a factor two to $400\,\mu$m.

5.4.3 Conclusions on HERA I alignment and calibration

The choice of the correct frame of reference is of greatest importance. In this respect robustness is more important than a possible gain in resolution as unforeseen systematic effects may lead to bad surprises. At the end all sub-detectors and projections should be aligned and calibrated simultaneously. Although this increases complexity it leads to more stable and unbiased results since all the correlations are properly taken into account.

5.5 Improvements for HERA II running

Thanks to the experience gained with *Millepede* during HERA I a number of improvements were introduced for HERA II data taking.
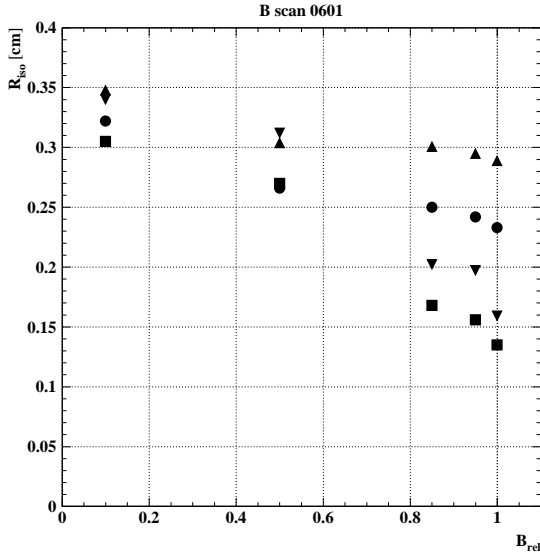

Fig. 5.5: CJC isochrone radius in centimetres as a function of relative magnetic field. For values of less than half of the nominal field an asymmetry due to the anode wire staggering is visible. For larger values the asymmetries in the sign of β are dominating. The trivial geometric value is 0.43 cm.

5.5.1 Millepede running online

At HERA II *Millepede* is also used for the online calibration of the main time-dependent CJC parameters $(v_\mathrm{d}, \alpha_\mathrm{lor})$. Calibration constants in the database are defined per H1 run, which typically lasts for about one hour. Thus a run is considered as a sample of events

taken with *constant* conditions. The online processing of the data is done on many processors in parallel as part of the offline reconstruction. Special data records with monitoring information like the *Millepede* linear equation system are inserted into the data stream by each processor. After the run end they are collected by a special job and a global fit is performed. When significant changes of the parameters occur the database is updated and the values are immediately fed back to the online processing of the following runs.

A similar scheme is also used to update the CJC calibration constants used by the fitter (DSPs) of the H1 track trigger [5].
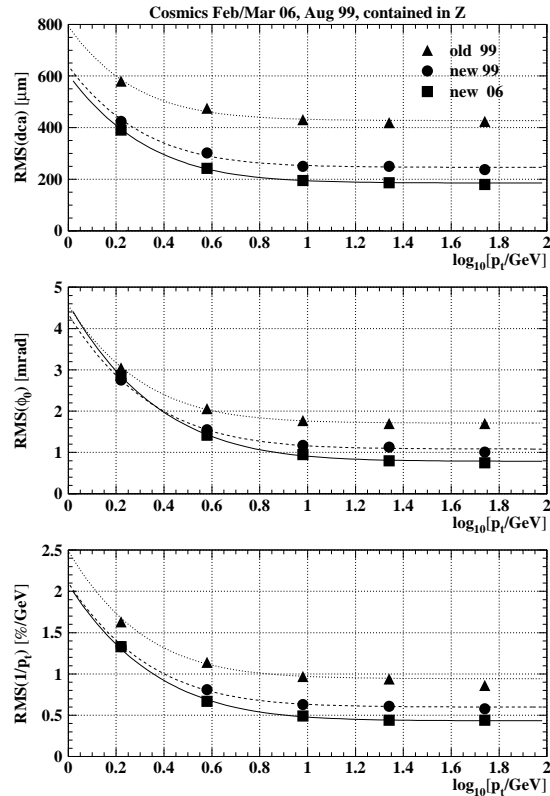

Fig. 5.6: CJC track parameter resolution in $R\varphi$ deduced from the comparison of cosmic track halves. As a function of the transverse momentum (p_t) from 1 to 100 GeV, the resolution in distance to the interaction point (d_ca), the angle at the interaction point (φ_0), and the curvature ($1/p_\mathrm{t}$) are shown. The upper curve represents results before alignment and calibration with *Millepede*, the middle one from afterwards, and the lower one from the recent improvements made at HERA II.

5.5.2 CJC calibration

The following refinements for the CJC calibration have been introduced recently.

– Inspired by a simulation with GARFIELD [6] the isochrone model has been improved. The isochrone radius depends now on the local magnetic field and is determined separately for the quadrants defined by the two drift sides and the signs of the angle β between normal to drift and flight direction (see Fig. 5.5).

– Radial variations of the electrical field are now reflected not only in corrections to the drift velocity (Δv_{d}) but also in corrections to the Lorentz angle ($\Delta \alpha_{\mathrm{lor}}$).

– The radial and longitudinal variations of the magnetic field ($B(R,Z)$) lead to corresponding dependencies of v_{d} and α_{lor}.

These modifications lead to the following changes in the time-to-distance relation:

$$
\begin{aligned}
d &= (t - t_0)V_{\mathrm{d}} + R_{\mathrm{iso\_quad}}(B)(\frac{1}{\cos\beta} - 1) \\
V_{\mathrm{d}} &= v_{\mathrm{d}}[1 + \Delta v_{\mathrm{d}}(R,Z) + \Delta\alpha_{\mathrm{lor}}(R,Z) \cdot \tan\beta] \, .
\end{aligned}
$$

As the CJC has operated until now during the HERA II running (2002–2006) without any problems, the resulting azimuthal variations are marginal.

With these modifications an overall improvement factor of two has been achieved for the track parameter resolution at high momenta (see Fig. 5.6). For momenta above several 10 GeV where the contribution from multiple scattering can be neglected, a resolution for the distance of closest approach of $185\,\mu$m, for the angle at the interaction point of 0.79 mrad and for the curvature ($1/p_{\mathrm{t}}$) of $0.43\,\%$/GeV has been measured by comparing cosmic track halves.

5.5.3 CST alignment

In the HERA II configuration the central part of the beam pipe has an elliptical shape to leave space for the synchrotron radiation fan. The CST had been reassembled to account for this new geometry and now also follows an elliptical shape. Therefore the alignment had to be redone from scratch. For all of the 192 silicon sensors two displacements in $R\varphi$ and three rotation angles have been determined. The method used is technically different from *Millepede* but equivalent.

5.5.3.1 Internal alignment with triplets

The internal alignment is done with CST hit triplets. The CST has only two layers, but there are azimuthal overlaps of the half-ladders of about 1.5%. Using the track curvature measured by the CJC, triplets are built from penetrating cosmics and overlaps of ep tracks. The two outer hits define the track parameters φ_0 and d_{ca}. The deviation Δ of the middle hit with coordinates $(r_{\mathrm{m}}, \varphi_{\mathrm{m}})$ from this track and the corresponding

error contribute to the χ^2 which has to be minimized.

$$
\Delta = \frac{\kappa}{2}(r_{\mathrm{m}}^2 + d_{\mathrm{ca}}^2) + (1 - \kappa d_{\mathrm{ca}})r_{\mathrm{m}} \sin(\varphi_0 - \varphi_{\mathrm{m}}) - d_{\mathrm{ca}}
$$
(5.3)

The analytic partial derivatives of this χ^2 with respect to all alignment parameters of the hits from a triplet are calculated and linearized to build a linear equation system for the 960 parameters. Linearization and outlier rejection requires some iterations. The large matrix is inverted by singular value decomposition for data sets of millions of ep overlaps and hundreds of thousands of cosmics. Constraints are not implemented. Instead one sensor is chosen as reference. For vertical incidence to the sensors a triplet resolution of $14\,\mu$m (see Fig. 5.7) has been achieved. This corresponds to the design single-hit resolution of $11\,\mu$m.
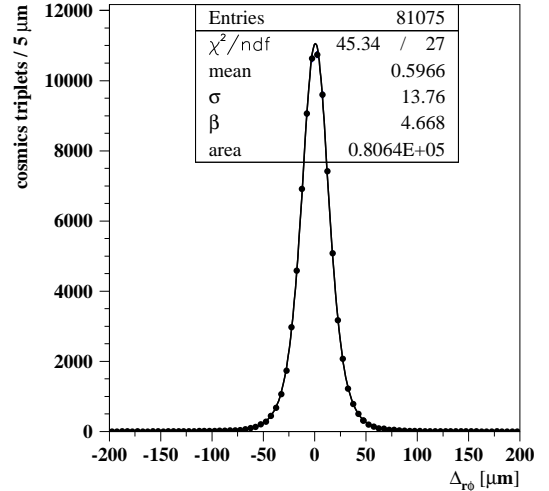

Fig. 5.7: CST triplet resolution for cosmics with nearly vertical incidence and p_{t} above 6 GeV after internal and external sensor alignment

5.5.3.2 External alignment to CJC

This method uses the CST as a rigid body and determines the alignment in $R\varphi$ with respect to the CJC. It is especially used to check the time stability of the alignment. Tracks from ep or cosmic tracks with two hits in the CST are used. Keeping the curvature from the CJC the track is forced through the CST hits. The deviation of these track parameters from those obtained from CJC alone and the corresponding errors and correlations enter the calculation of χ^2, which is minimized as for the internal alignment.

The method has been extended to determine alignment parameters for each sensor as in the case of

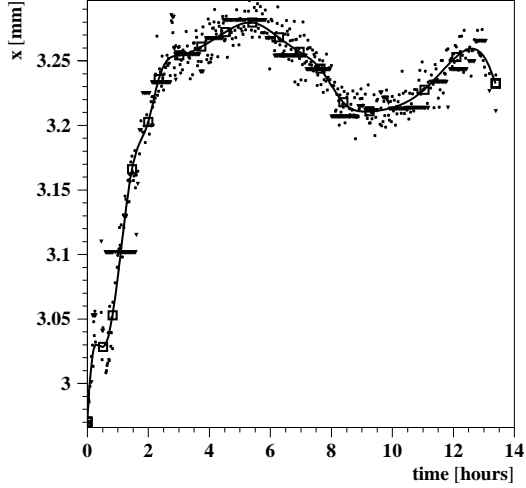the triplets. Finally the combination of the methods is used for the sensor alignment.

5.5.4 Stability monitoring

For offline monitoring of the CST and the beam position, samples of the order of a thousand selected tracks corresponding to about 10 minutes of running with ep collisions are used.

5.5.4.1 CST position

To check the CST versus the CJC for samples of four hundred tracks, the external alignment is performed and determines the position with an accuracy of about $15\,\mu$m. For the 2005 data taking, in each luminosity fill lasting about 8–12 hours a systematic drift of a few microns per hour probably due to temperature effects has been observed. After improving the mounting of the CST in 2006 the stability is better than a few microns per week.

5.5.4.2 Beam position

For some subset of ep data the average transverse beam position $(x_{\mathrm{v}}, y_{\mathrm{v}})$ is determined from the azimuthal dependence of the distance of closest approach.

$$d_{\mathrm{ca}} = x_{\mathrm{v}} \sin \varphi_0 - y_{\mathrm{v}} \cos \varphi_0 \; . \qquad (5.4)$$

For the CJC with a resolution in this distance of a few hundred microns this is done only once per H1 run in order to achieve the required precision. The CST with the superior resolution can do this for the samples of a few thousand tracks. At the beginning of a luminosity fill typically fast drifts are observed and slower drifts during the run of the order of one hundred microns due to temperature effects and occasionally 'arbitrary' jumps due to beam steering (see Fig. 5.8). This variation in time is parameterized for each luminosity run by cubic B-splines with adaptive nodes [7]. Thus beam movements can be followed with a precision of about 10 μm.

The quality of the alignment and beam position measurement can be checked by comparing the measured and expected resolution of the distance of closest approach of the tracks to the beam position. Taking into account the transverse beam spot size as calculated from beam emittance and divergence, good agreement has been achieved (see Fig. 5.9).
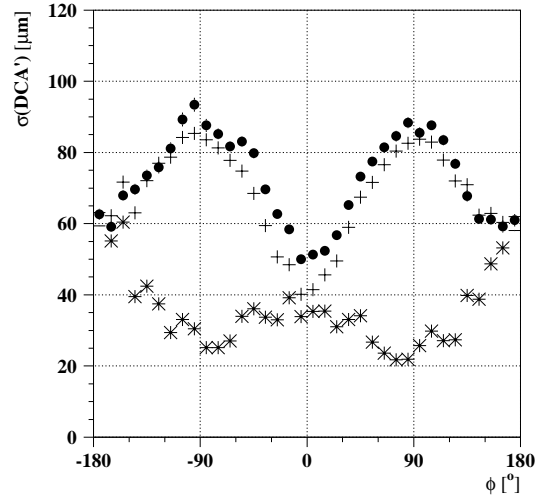

Fig. 5.9: Resolution of d_{ca} for p_{t} above 6 GeV in microns as a function of φ_0 for the 2006 e^- running. The dots are the measurement, the stars the contribution from the CST intrinsic resolution and multiple scattering. The crosses include in addition the expected beam size of $80\,\mu$m in x and $20\,\mu$m in y.

5.6 Summary

With *Millepede* and compatible methods, great improvements in the alignment and calibration of the H1 central drift chambers and central silicon strip detectors have been achieved. This concerns monitoring of time stability as well as complex detailed local corrections.

Acknowledgments

References

[1] H1 Collaboration, *Nucl. Instrum. Methods* **A386** (1997) 310–396.

[2] D. Pitzl *et al.*, *Nucl. Instrum. Methods* **A454** (2000) 334–349.

[3] V. Blobel and C. Kleinwort, *A new method for the high-precision alignment of track detectors*, PHYSTAT2002, Durham [`arXiv:hep-ex/0208021`].

[4] C. Niebuhr, *Nucl. Instrum. Methods* **A515** (2003) 43–49.

[5] A. Baird *et al.*, *IEEE Trans. Nucl. Sci.* **48** (2001) 1276 [`arXiv:hep-ex/0104010`].

[6] R. Veenhof, *GARFIELD: a drift chamber simulation program*, CERN program library W5050.

[7] Paul Dierckx, *Curve and surface fitting with splines* (Clarendon Press, Oxford, 1993).